Catalysis Letters Vol. 81, No. 3–4, August 2002 (©2002)

Kinetic aspects of the structure-gap problem in heterogeneous catalysis

V.P. Zhdanov [a,b,*] and B. Kasemo [a]

[a] *Department of Applied Physics, Chalmers University of Technology, S-41296 Göteborg, Sweden*
[b] *Boreskov Institute of Catalysis, Russian Academy of Sciences, Novosibirsk 630090, Russia*

Received 20 November 2001; accepted 7 March 2002

Analyzing one of the possible schemes of the NO–CO reaction occurring on nm-sized supported Rh or Pd particles, we show that, due to the purely kinetic effects related to the interplay of the reaction kinetics on the (111) and (100) facets, the activity of a catalyst particle may be appreciably higher than that calculated by using the conventional approximation based on the assumption that the facets operate independently. The dependence of the turnover reaction rate on the fraction of adsorption sites belonging to the (100) facet is found to exhibit a broad maximum at $f \simeq 0.4$.

KEY WORDS: nm-sized supported crystallites; structure-gap problem; structure sensitivity; NO–CO reaction; rhodium; palladium.

In practice, heterogeneous catalytic reactions frequently run on very small supported crystalline particles, in the nanometer range ($\lesssim 10\,\mathrm{nm}$) [1]. The specific catalytic activity (per adsorption site) of such particles is often quite different compared with that of single-crystal samples employed in academic studies. The collective set of such differences and the challenge to understand and explain them is referred to as the "structure-gap problem" in catalysis. The physics behind this gap is usually associated with unique electronic properties of nm-sized metal particles, with the contribution of special sites, such as edges, to the reaction rate, and/or with metal–support interaction [2]. The structure gap may, however, also be due to purely kinetic effects [3], such as the interplay of the reaction kinetics occurring on different communicating facets. This was recently explicitly illustrated by analyzing the kinetics of CO and C_3H_8 oxidation [4,5] running on nm-supported Pt particles, containing (111) and (100) facets. In both these cases, the reaction rate depends on the balance between the adsorption rates of CO or C_3H_8 and O_2. If the reactant sticking coefficients on different facets are different, and if there is communication between facets by adsorbate diffusion, the total reaction kinetics are far from those calculated as the sum of the kinetics of separate, non-interacting facets (the latter way of calculating the catalytic activity of nm particles is common). The goal of this letter is to show that the interplay of the reaction kinetics occurring on different facets may lie behind the structure gap also in more complex cases. Specifically, we treat a model describing the generic case when the reaction rate is influenced by product desorption.

As an example, we analyze one of the most probable reaction schemes of the NO–CO reaction occurring on such metals as Rh and Pd [6–9],

$$A_{\mathrm{gas}} \rightleftharpoons A_{\mathrm{ads}} \tag{1}$$

$$B_{\mathrm{gas}} \rightleftharpoons B_{\mathrm{ads}} \tag{2}$$

$$A_{\mathrm{ads}} \rightarrow C_{\mathrm{ads}} + D_{\mathrm{ads}} \tag{3}$$

$$B_{\mathrm{ads}} + D_{\mathrm{ads}} \rightarrow (BD)_{\mathrm{gas}} \tag{4}$$

$$2C_{\mathrm{ads}} \rightarrow (C_2)_{\mathrm{gas}} \tag{5}$$

where A and B stand for NO and CO, and C and D represent N and O.

The reaction above is assumed to occur on a nm-sized particle containing primarily (111) and (100) facets (figure 1). In general, the reaction kinetics on such particles should be analyzed by using the Monte Carlo technique [3]. If, however, (i) the particle size is not too small (*e.g.*, $\sim 10\,\mathrm{nm}$), (ii) the reaction is not accompanied by phase separation of adsorbates, and (iii) reactant mobility is high, one can employ the mean-field (MF) kinetic equations. In our MF treatment, we focus on the interplay of the reaction kinetics on the (111) and (100) facets. Taking into account that many details of the NO–CO reaction on the (111) and (100) faces of Rh and Pd are still ambiguous, we did not attempt to construct a comprehensive model of this reaction on the nm scale. Our goal is rather to show one of the possible reaction scenarios exhibiting interesting and instructive features. To simplify the analysis, we ignore such complications as adsorbate–adsorbate lateral interactions, adsorption of different species on different sites, contribution of edges, and NO and CO supply via the support. In reality, all these factors may be important, but they are not crucial for our general conclusions.

---

[*] To whom correspondence should be addressed.

1011-372X/02/0800-0141/0 © 2002 Plenum Publishing Corporation

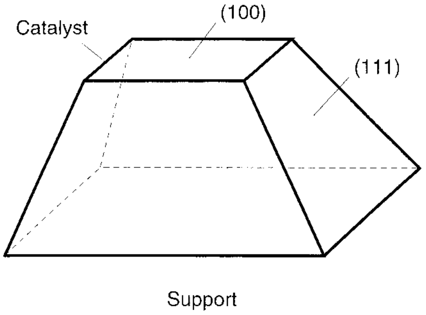

Figure 1. Schematic structure of a supported catalyst particle.

To make the presentation transparent, we take into account the specifics of the steady-state kinetics of the NO–CO reaction. (i) Steps (1) and (2) are considered to be rapid so that the adsorbed and gas-phase A and B species are in equilibrium. (ii) Step (4) is assumed to be so fast that the D particles are removed from the surface immediately after formation. This means that the D coverage is negligible, *i.e.*, we need to operate only with the A, B and C coverages. (iii) The adsorption and desorption rate constants for A are taken to be equal to those for B. This approximation makes sense, because numerous temperature-programmed-desorption experiments indicate that CO desorption from Pd and Rh usually occurs at the same temperatures, 400–500 K, as NO desorption; the density-functional theory (DFT) [10] also predicts that the difference of the CO and NO binding energies on Pd is small, about 0.1 eV. In addition, A and B adsorption is assumed to be structure-insensitive, *i.e.*, the A and B adsorption and desorption rate constants, $k_{\rm ad}$ and $k_{\rm des}$, are considered to be independent of the arrangement of the metal atoms on the facets. The latter approximation is reasonable, because the difference in the energetics of CO and NO adsorption on the (111) and (100) faces is minor compared with that of N. (iv) The reaction is assumed to run at equal A and B pressures.

With the specification above, there is no difference between communicating and non-communicating facets due to adsorption kinetics (*e.g.*, sticking coefficients) or desorption kinetics of the initial reactants A and B, as in refs. [3]–[5]. Thus, the novel effects, demonstrated below, instead originate from the differences on the two facets in the kinetics of A dissociation and C desorption.

The steady-state A and B coverages of the (111) and (100) facets, θ_A and θ_A^*, and the corresponding fractions of vacant sites, $\theta_{\rm v}$ and $\theta_{\rm v}^*$, are given in both cases (with and without communication) by the conventional Langmuir expressions,

$$\theta_A = \theta_B = \frac{(1-\theta_C)k_{\rm ad}P}{k_{\rm des}+2k_{\rm ad}P} \tag{6}$$

$$\theta_A^* = \theta_B^* = \frac{(1-\theta_C^*)k_{\rm ad}P}{k_{\rm des}+2k_{\rm ad}P} \tag{7}$$

$$\theta_{\rm v} = \frac{(1-\theta_C)k_{\rm des}}{k_{\rm des}+2k_{\rm ad}P} \tag{8}$$

$$\theta_{\rm v}^* = \frac{(1-\theta_C^*)k_{\rm des}}{k_{\rm des}+2k_{\rm ad}P} \tag{9}$$

where θ_C is the C coverage, and P is the A or B pressure (the superscript $*$ is here and below associated with the (100) facet).

If the reaction occurs on the kinetically independent (non-communicating) (111) and (100) facets of a catalyst particle (or on the (111) and (100) faces of a single-crystal sample), we have in addition two equations describing the balance of the rates of C formation and removal (steps (3) and (5)),

$$\mathcal{K}_{\rm dis}\theta_A\theta_{\rm v} = \mathcal{K}_{\rm des}\theta_C^2 \tag{10}$$

$$\mathcal{K}_{\rm dis}^*\theta_A^*\theta_{\rm v}^* = \mathcal{K}_{\rm des}^*(\theta_C^*)^2 \tag{11}$$

where $\mathcal{K}_{\rm dis}$, $\mathcal{K}_{\rm des}$, $\mathcal{K}_{\rm dis}^*$ and $\mathcal{K}_{\rm des}^*$ are the dissociation and desorption rate constants. Combining equations (6)–(11) yields

$$\frac{\theta_C}{1-\theta_C} = \left[\frac{\mathcal{K}_{\rm dis}k_{\rm des}k_{\rm ad}P}{\mathcal{K}_{\rm des}(k_{\rm des}+2k_{\rm ad}P)^2}\right]^{1/2} \tag{12}$$

$$\frac{\theta_C^*}{1-\theta_C^*} = \left[\frac{\mathcal{K}_{\rm dis}^*k_{\rm des}k_{\rm ad}P}{\mathcal{K}_{\rm des}^*(k_{\rm des}+2k_{\rm ad}P)^2}\right]^{1/2} \tag{13}$$

Using the latter two formulae makes it straightforward to obtain explicit expressions for all the coverages and reaction rates.

If the (111) and (100) facets are communicating by rapid diffusion, the balance of the rates of C formation and removal is given by

$$n\mathcal{K}_{\rm dis}\theta_A\theta_{\rm v} + n^*\mathcal{K}_{\rm dis}^*\theta_A^*\theta_{\rm v}^* = n\mathcal{K}_{\rm des}\theta_C^2 + n^*\mathcal{K}_{\rm des}^*(\theta_C^*)^2 \tag{14}$$

where n and n^* are the corresponding numbers of adsorption sites. In addition, applying the detailed balance principle to the distribution of C particles, we obtain

$$\theta_C^*(1-\theta_C) = \theta_C(1-\theta_C^*)\exp(\Delta E_{\rm a}/k_{\rm B}T) \tag{15}$$

or

$$\theta_C^* = \frac{\theta_C\exp(\Delta E_{\rm a}/k_{\rm B}T)}{1-\theta_C+\theta_C\exp(\Delta E_{\rm a}/k_{\rm B}T)} \tag{16}$$

where $\Delta E_{\rm a}$ is the difference of the C binding energies on the (100) and (111) facets ($\Delta E_{\rm a} > 0$ if the binding energy is larger on the (100) facet). Employing equations (6)–(9), (14) and (16), one can easily calculate all the coverages and reaction rates, including the average reaction turnover rate, defined as

$$W = (1-f)\mathcal{K}_{\rm dis}\theta_A\theta_{\rm v} + f\mathcal{K}_{\rm dis}^*\theta_A^*\theta_{\rm v}^* \tag{17}$$

where $f = n^*/(n+n^*)$ is the fraction of adsorption sites belonging to the (100) facet.

To analyze the reaction kinetics, it is convenient to relate the rate constants for A dissociation on the (111) and (100) facets *via* the corresponding Arrhenius parameters. Neglecting in this case the variation in the pre-exponential factors, we have

$$\mathcal{K}_{\mathrm{dis}}^{*} = \mathcal{K}_{\mathrm{dis}} \exp(\Delta E_{\mathrm{dis}}/k_{\mathrm{B}}T) \tag{18}$$

where ΔE_{dis} is the difference in the dissociation activation energies. For C_2 desorption, a similar relation is

$$\mathcal{K}_{\mathrm{des}}^{*} = \mathcal{K}_{\mathrm{des}} \exp(\Delta E_{\mathrm{des}}/k_{\mathrm{B}}T) \tag{19}$$

where ΔE_{des} is the difference in the desorption activation energies. (If the barriers for C_2 (N_2) adsorption on the (111) and (100) facets were equal, one could relate ΔE_{a} and ΔE_{des}. In reality, C_2 adsorption is, however, expected to be structure sensitive, and one cannot express ΔE_{des} *via* ΔE_{a}.)

The kinetic equations above depend only on the dimensionless ratios of the rate constants. In the calculations, we employ $k_{\mathrm{des}}/k_{\mathrm{ad}}P = 0.1$. With this choice, the surface is almost completely covered by NO and CO (provided that there is no reaction). The ratio $\mathcal{K}_{\mathrm{dis}}/\mathcal{K}_{\mathrm{des}}$ is varied over a wide range (from 0.1 to 10) in order to illustrate what may happen in different situations. For the energetic parameters, we use the DFT values [10], $\Delta E_{\mathrm{a}} \simeq 0.1\,\mathrm{eV}$, $\Delta E_{\mathrm{dis}} \simeq 0.4\,\mathrm{eV}$ and $\Delta E_{\mathrm{des}} \simeq -0.1\,\mathrm{eV}$, obtained for the NO–CO/Pd system. Assuming $T \simeq 500\text{–}700\,\mathrm{K}$, we set $\Delta E_{\mathrm{a}}/k_{\mathrm{B}}T = 2$, $\Delta E_{\mathrm{dis}}/k_{\mathrm{B}}T = 8$ and $\Delta E_{\mathrm{des}}/k_{\mathrm{B}}T = -2$.

The average reaction turnover rate (equation (17)) was calculated for a catalyst particle with kinetically independent and communicating facets (with $f = 0.2$), *i.e.*, (i) by using the conventional approximation based on the assumption that the (111) and (100) facets operate independently (equations (6)–(13), and (ii) by taking into account the interplay of the reactions on different facets (equations (6)–(9), (14) and (16)). In the latter case, the turnover rate is found to be appreciably (by a factor of 5) higher (figure 2). To explain the physics behind this finding, we show (figure 3) for the two cases the C coverage and A-dissociation rates (per site) on the (111) and (100) facets. In the case of kinetically independent (111) and (100) facets, the corresponding coverages are low and high, because on the (100) facet the rate constants for A dissociation and C_2 desorption are, respectively, higher and lower than those on the (111) facets (both these factors result in higher C coverage on the (100) facet). If the facets communicate, the C coverage of the (100) and (111) facet becomes lower and higher, respectively, because C particles may diffuse from the (100) facet to the (111) facets. This results in an increase of the fraction of vacant sites and accordingly of the A-dissociation rate on the (100) facet. The rate of C_2 desorption on this facet decreases. Simultaneously, the fraction of vacant sites and the A-dissociation rate on the (111) facets decrease. The rate of C_2 desorption on the latter facet increases. The net effect of these changes is positive, because the (100) facet is catalytically more active. (Note that globally the rates of A dissociation and C_2 desorption should be balanced. In our example, an increase in the A-dissociation rate on the (100) facet is equated by an increase in the C_2-desorption rate on the (111) facets.)

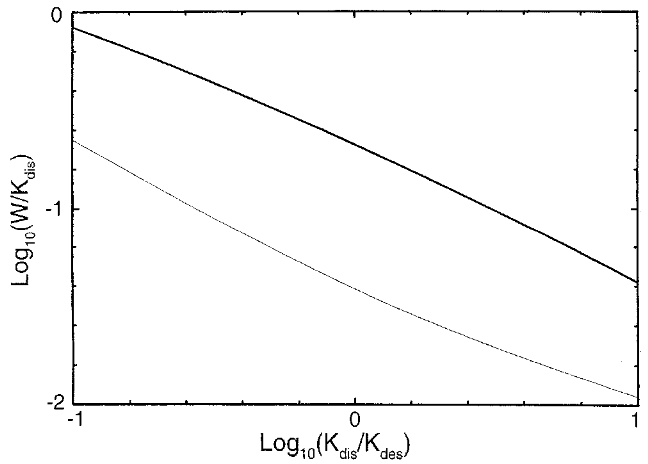

Figure 2. Average reaction turnover rate (normalized to $\mathcal{K}_{\mathrm{dis}}$) as a function of the ratio $\mathcal{K}_{\mathrm{dis}}/\mathcal{K}_{\mathrm{des}}$ for a catalyst particle with $f = 0.2$. The thick line is for the case where the model takes into account the interplay of the reactions on the (111) and (100) facets. The thin line corresponds to the conventional approximation based on the assumption that the (111) and (100) facets operate independently.

Scrutinizing the arguments above, we may note that the increase of the average turnover rate on a catalyst particle is connected with the fact that the limiting reaction steps on separate (111) and (100) facets are

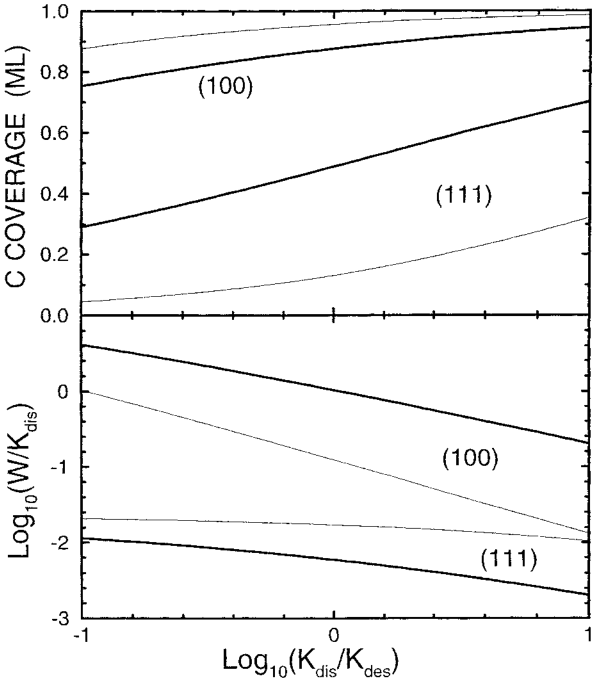

Figure 3. C coverage and A-dissociation rate (per site) on the (111) and (100) facets. The thick lines are for the communicating facets. The thin lines correspond to the (111) and (100) facets operating independently.

different (the reaction is limited by NO dissociation and N_2 desorption, respectively). Changing the model parameters or increasing pressure, one can easily obtain the situation where the reaction rate on the facets of both types is limited by NO dissociation. In the latter case, the N coverage will be relatively low on all the facets, the effect of communication between the facets due to N diffusion will be negligible, and accordingly the reaction rate on a catalyst particle will be nearly equal to that on separately operating facets. In principle, the average turnover rate on a catalyst particle with communicating facets may be lower than that calculated by ignoring the facet–facet communication. Our experience indicates, however, that for the model under consideration this can hardly be realized.

The equilibrium geometric shape of nm catalyst particles is determined by the Wulff rule, stating that the shape is a consequence of minimizing the total surface free energy. Practically, this means that catalyst particles of fcc metals contain primarily the (111) facets and partly the (100) facets. In reality, catalyst particles often do not reach equilibrium and accordingly the relative area of the (100) facets may be larger than that corresponding to equilibrium (especially in the case of model-supported catalysts [12–14] fabricated under conditions far from equilibrium). Bearing in mind this point, we have calculated (figure 4) the average reaction turnover rate as a function of f for the whole range of f values. In this case, our model predicts a broad maximum in the reaction rate at $f \simeq 0.4$. With our model parameters, this ratio is optimal for the balance of the rates of A-dissociation rate on the (100) facet and C_2-desorption rate on the (111) facets.

Finally, it is appropriate to comment on the applicability of our results to specific systems, *i.e.*, to the NO–CO reaction on Rh and Pd:

(i) The accepted mechanism of the NO–CO reaction (steps (1)–(5)) is open for debate even in the case of single crystals (see, *e.g.*, refs. [9,15,16]). At present, we cannot exclude that on single-crystal surfaces or especially on supported catalyst particles the reaction includes some additional steps influencing the reaction kinetics.

(ii) A detailed full-scale analysis of these systems was beyond our present goals. Instead, we tried to identify a representative set of the model parameters for a more restricted analysis. The most important (energetic) parameters were taken from DFT calculations [10] performed for the NO–CO/Pd system in the low-coverage limit. We employed these parameters at high coverages and there is therefore no guarantee that these parameters are good in the latter case or in the case of Rh.

(iii) Diffusion of all the adsorbed species was assumed to be fast. For NO and CO molecules, this is obviously the case. The situation with diffusion of N atoms is, however, not so straightforward. The DFT calculations [11] indicate that the activation barriers for N diffusion on the (111) and (100) faces of Pd are 0.80 (0.84) eV and 1.03 (1.11) eV, respectively (the two values for each face correspond to the GGA-RPBE and GGA-PW91 functionals). For the (111) and (100) faces of Rh, the corresponding values are 0.51 (0.56) eV and 0.63 (0.69) eV. These barriers are appreciable, but as we expected they are lower than the barriers for N_2 desorption. Thus, these data are in favor of our model. On the other hand, recent studies [17] of the kinetics of the NO–CO reaction on Rh(111) indicate that N diffusion may be slow. Here we may notice that the NO–CO reaction in the case of Rh(111) may primarily occur on steps, because the activation barrier for NO dissociation on steps seems to be much lower than on the (111) terraces [10]. Therefore, the kinetic effects

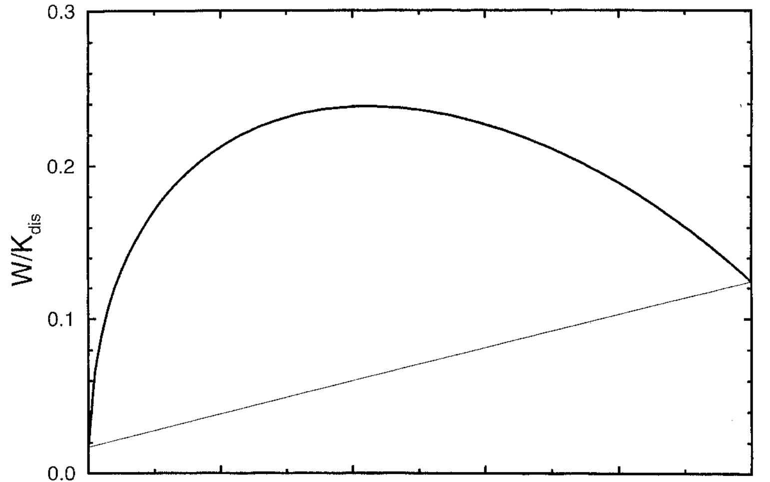

Figure 4. Average reaction turnover rate as a function of f for $\mathcal{K}_{dis}/\mathcal{K}_{des} = 1$ in the cases of communicating (thick line) and kinetically independent (thin line) facets.

observed in ref. [17] may be connected with N diffusion from steps to terraces, and accordingly the conclusions drawn there may be inapplicable to small nm-sized catalyst particles.

(iv) We ignored the contribution of edges. This appears reasonable, because according to ref. [10] the activation energy for NO dissociation on edges is the same as on the (100) face.

Despite the limitations above, we believe that the qualitative results obtained in our study are generic. In summary, our calculations indicate that due to purely kinetic factors related to the interplay of the reaction kinetics on different facets the activity of a catalyst particle may be appreciably higher than that calculated by assuming that the facets operate independently. Specifically, our analysis identifies the conditions favourable for observations of this effect. First of all, reactions should be structure-sensitive. Secondly, the species participating in the rate-determining step should run far from the adsorption–desorption equilibrium. Both these conditions are often met in reality.

Acknowledgments

We thank B. Hammer for presenting us with the unpublished results of his DFT calculations of the activation barriers for N diffusion on Pd and Rh and for useful discussions. This work was supported by the NUTEK Competence Center for Catalysis at Chalmers University of Technology (grant No. 4F7-97-10929).

References

[1] J.M. Thomas and W.J. Thomas, *Principles and Practice of Heterogeneous Catalysis* (VCH, Weinheim, 1997).
[2] M. Che and C.O. Bennett, Adv. Catal. 36 (1989) 55.
[3] V.P. Zhdanov and B. Kasemo, Surf. Sci. Rep. 39 (2000) 25.
[4] V.P. Zhdanov and B. Kasemo, Surf. Sci. 405 (1998) 27.
[5] V.P. Zhdanov, Phys. Rev. B 64 (2001) 193406.
[6] H.F. Peden, D.N. Belton and S.J. Schmieg, J. Catal. 155 (1995).
[7] G.S. Herman, H.F. Peden, S.J. Schmieg and D.N. Belton, Catal. Lett. 62 (1999) 131.
[8] L. Piccolo and C.R. Henry, J. Mol. Catal. A 167 (2001) 181.
[9] V.P. Zhdanov and B. Kasemo, Surf. Sci. Rep. 29 (1997) 31.
[10] B. Hammer, J. Catal. 199 (2001) 171.
[11] B. Hammer, unpublished results (private communication).
[12] P.L.J. Gunter, J.W. Niemantsverdriet, F.H. Ribeiro and G.A. Somorjai, Catal. Rev. Sci. Eng. 39 (1997) 77.
[13] C.R. Henry, Surf. Sci. Rep. 31 (1998) 231.
[14] H.-J. Freund, M. Baumer and H. Kuhlenbeck, Adv. Catal. 45 (2000) 333.
[15] S.M. Vesecky, D.R. Rainer and D.W. Goodman, J. Vac. Sci. Techn. A 14 (1996) 1457.
[16] C.S. Gopinath and F. Zaera, J. Catal. 200 (2001) 270.
[17] F. Zaera, S. Wehner, C.S. Gopinath, J.L. Sales, V. Gargiulo and G. Zgrablich, J. Phys. Chem. B 105 (2001) 7771.